

A Saddle Point Approach to Structured Low-rank Matrix Learning

Pratik Jawanpuria* Bamdev Mishra*

October 13, 2021

Abstract

We propose a novel optimization approach for learning a low-rank matrix which is also constrained to lie in a linear subspace. Exploiting a particular variational characterization of the squared trace norm regularizer, we formulate the structured low-rank matrix learning problem as a rank-constrained saddle point minimax problem. The proposed modeling decouples the low-rank and structural constraints onto separate factors. The optimization problem is formulated on the Riemannian spectrahedron manifold, where the Riemannian framework allows to propose computationally efficient conjugate gradient and trust-region algorithms. Our approach easily accommodates popular non-smooth loss functions, e.g., ℓ_1 -loss, and our algorithms are scalable to large-scale problem instances. The numerical comparisons show that our proposed algorithms outperform state-of-the-art algorithms in standard and robust matrix completion, stochastic realization, and multi-task feature learning problems on various benchmarks.

1 Introduction

Low-rank matrices are commonly learned in several machine learning applications such as matrix completion (Candès & Recht, 2009), multi-task learning (Argyriou et al., 2006, 2008; Amit et al., 2007), multivariate regression (Yuan et al., 2007; Journée et al., 2010), to name a few. In addition to the low-rank constraint, other structural constraints may exist, e.g., entry-wise *non-negative* (Kannan et al., 2014) and *bounded* constraints (Marecek et al., 2017). Several linear dynamical system models require learning a low-rank *Hankel* matrix (Fazel et al., 2013; Markovsky & Usevich, 2013). Hankel matrix has the structural constraint that all its anti-diagonal entries are same. In robust matrix completion (Candès & Plan, 2009) and robust PCA (Wright et al., 2009) problems, the matrix is learned as a superimposition of a low-rank matrix and a sparse matrix. This sparse structure is modeled effectively by choosing the loss function as the ℓ_1 -loss (Cambier & Absil, 2016). Low-rank 1-bit matrix completion solvers employ the *logistic* loss function (Davenport et al., 2014; Bhaskar & Javanmard, 2015).

Our focus in this paper is on learning structured low-rank matrices with the formulation

$$\min_{\mathbf{W} \in \mathbb{R}^{d \times T}} \frac{1}{2} R(\mathbf{W}) + CL(\mathbf{W}, \mathbf{Y}), \quad \text{subject to } \mathbf{W} \in \mathcal{D}, \quad (1)$$

where $\mathbf{Y} \in \mathbb{R}^{d \times T}$ is a given matrix, $L : \mathbb{R}^{d \times T} \times \mathbb{R}^{d \times T} \rightarrow \mathbb{R}$ is a loss function, R is a low-rank promoting regularizer, $C > 0$ is the cost parameter, and \mathcal{D} is the *linear* subspace corresponding to structural constraints.

*Core Machine Learning Team, Amazon.com, Bengaluru 560055, India (e-mail: jawanpur,bamdevm@amazon.com).

The approach in (Fazel et al., 2013) uses $R(\mathbf{W}) = \|\mathbf{W}\|_*$ in (1) to learn a Hankel matrix (enforced by \mathcal{D}) with the alternating direction method of multipliers approaches. $\|\mathbf{W}\|_*$ is the trace (nuclear) norm, which is the sum of the singular values of \mathbf{W} . The trace norm regularizer promotes low-rank solutions. (Yu et al., 2014) also uses $\|\mathbf{W}\|_*$ as low-rank regularizer for learning Hankel matrices, but relaxes the strict structural constraint with a penalty term in the objective function. They propose a generalized gradient algorithm. Instead of employing $R(\mathbf{W})$ in (1), (Markovsky & Usevich, 2013) learns a Hankel matrix by fixing the rank *a priori* and strictly enforcing the structural constraints.

Without the $\mathbf{W} \in \mathcal{D}$ constraint, the works (Toh & Yun, 2010; Hsieh & Olsen, 2014) propose singular value thresholding and active learning algorithms for (1) when the low-rank regularizer is $\|\mathbf{W}\|_*$. Fixed-rank approaches (Cambier & Absil, 2016; Boumal & Absil, 2011; Wen et al., 2012; Mishra et al., 2013; Vandereycken, 2013; Mishra & Sepulchre, 2014; Boumal & Absil, 2015; Tan et al., 2016) tackle low-rank learning problems (without the structural constraint) by fixing the rank explicitly. They differ in the scheme of factorization, the loss function L , and the algorithm to solve (1). For example, (Wen et al., 2012) propose alternate least-squares algorithms (and variants) specifically for the matrix completion problem with the square loss function. The works (Boumal & Absil, 2011; Mishra et al., 2013; Vandereycken, 2013; Mishra & Sepulchre, 2014; Boumal & Absil, 2015) exploit the Riemannian geometry of fixed-rank matrices and propose a number of first- and second-order algorithms for smooth L . (Cambier & Absil, 2016) employs the pseudo-Huber loss as a proxy for the non-smooth ℓ_1 -loss in robust matrix completion. The issue of tuning the rank for fixed-rank approaches is discussed in (Journée et al., 2010; Wen et al., 2012; Mishra et al., 2013; Tan et al., 2016). The problem (1) is well studied for $R(\mathbf{W}) = \|\mathbf{W}\|_*^2$ in the convex multi-task feature learning framework without the $\mathbf{W} \in \mathcal{D}$ constraint (Argyriou et al., 2006, 2008; Zhang & Yeung, 2010; Jawanpuria & Nath, 2011; Ciliberto et al., 2015).

We propose a *generic* saddle point approach to the structured low-rank matrix learning problem (1) that is well suited for handling a variety of loss functions L (e.g., ℓ_1 -loss and ϵ -SVR loss) and structural constraints \mathcal{D} and is scalable for large-scale problem instances. Our approach for (1) exploits a well-studied *variational* characterization of $\|\mathbf{W}\|_*^2$ (Argyriou et al., 2006, 2008) to propose a *novel* rank-constrained minimax problem formulation for (1).

In particular, our formulation allows to learn a rank- r structured matrix \mathbf{W} as $\mathbf{W} = \mathbf{U}\mathbf{U}^\top(\mathbf{Z} + \mathbf{A})$, where $\mathbf{U} \in \mathbb{R}^{d \times r}$ and $\mathbf{Z}, \mathbf{A} \in \mathbb{R}^{d \times T}$. Our factorization naturally decouples the low-rank and structural constraints on \mathbf{W} . The low-rank of \mathbf{W} is enforced with \mathbf{U} , the structural constraint $\mathbf{W} \in \mathcal{D}$ is modeled by \mathbf{A} , and the loss function L is modeled by \mathbf{Z} . To the best of our knowledge, such a decoupling has not been studied in existing structured low-rank matrix learning works (Fazel et al., 2013; Markovsky & Usevich, 2013; Cambier & Absil, 2016; Yu et al., 2014). The separation of low-rank and structural constraints onto separate factors make the optimization conceptually simpler. Our saddle point approach leads to an optimization problem on the Riemannian spectrahedron manifold (Journée et al., 2010). We exploit the Riemannian framework to propose computationally efficient conjugate gradient (first-order) and trust-region (second-order) algorithms.

The proposed algorithms outperform state-of-the-art algorithms in stochastic system realization problems for learning low-rank Hankel matrix, and standard and robust low-rank matrix completion problems. Our algorithms readily scale to the Netflix data set, even for the non-smooth ℓ_1 -loss and ϵ -SVR (ϵ -insensitive support vector regression) loss functions.

The outline of the paper is as follows. Section 2 introduces the saddle point approach to learn structured low-rank matrices and Section 3 presents our proposed formulation. The optimization methodology is discussed in Section 4. The empirical results are presented in Section 5. In Section 6, we present theoretical results related to the global optimality of our solution.

The proofs of all the theorems as well as additional experiments are provided in the supplementary material. The Matlab codes are available at <https://pratikjawanpuria.com/>.

2 Minimax Formulation for Structured Low-rank Matrix Learning

We present our formulations and derivations for the problem of learning a structured low-rank matrix \mathbf{W} close to a given matrix \mathbf{Y} . Let w_t denote the t^{th} column of \mathbf{W} and w_{ti} denote the i^{th} row of column w_t . The loss term $L(\mathbf{W}, \mathbf{Y})$ in (1) is defined as $L(\mathbf{W}, \mathbf{Y}) := \sum_{t=1}^T \sum_{i=1}^d l(y_{ti}, w_{ti})$, where $l : \mathbb{R} \times \mathbb{R} \rightarrow \mathbb{R}$ is a loss function convex in the second argument. The linear subspace \mathcal{D} in problem (1) is represented as $\mathcal{D} := \{\mathbf{W} : \mathcal{A}(\mathbf{W}) = \mathbf{0}\}$, where $\mathcal{A} : \mathbb{R}^{d \times T} \rightarrow \mathbb{R}^n$ is a linear map. The set of $d \times d$ positive semi-definite matrices with unit trace is denoted by \mathcal{P}^d . The pseudoinverse of a matrix Θ is represented as Θ^\dagger .

We begin with a well-known variational characterization of the squared trace norm regularizer.

Lemma 1. [Theorem 4.1 in (Argyriou et al., 2006)] Let $\text{range}(\Theta) = \{\Theta z : z \in \mathbb{R}^d\}$. The following results holds:

$$\|\mathbf{W}\|_*^2 = \min_{\Theta \in \mathcal{P}^d, \text{range}(\mathbf{W}) \subseteq \text{range}(\Theta)} \sum_{t=1}^T w_t^\top \Theta^\dagger w_t \quad (2)$$

For a given \mathbf{W} matrix, the optimal $\Theta^* = \sqrt{\mathbf{W}\mathbf{W}^\top} / \text{trace}(\sqrt{\mathbf{W}\mathbf{W}^\top})$.

Based on the above result, we study the following variant of problem (1) by taking the low-rank regularizer $R(\mathbf{W}) = \|\mathbf{W}\|_*^2$, i.e.,

$$\min_{\Theta \in \mathcal{P}^d} \sum_{t=1}^T \min_{w_t \in \mathbb{R}^d} \frac{1}{2} w_t^\top \Theta^\dagger w_t + C \sum_{i=1}^d l(y_{ti}, w_{ti}), \quad \text{subject to } \mathcal{A}(\mathbf{W}) = \mathbf{0}. \quad (3)$$

The above structured matrix learning formulation, shifts the low-rank constraint on \mathbf{W} to Θ . It should be noted that Lemma 1 guarantees that the rank of Θ and \mathbf{W} are equal at optimality. Problem (3), without $\mathcal{A}(\mathbf{W}) = \mathbf{0}$ constraint, has been studied in multi-task learning setup in (Argyriou et al., 2006, 2008; Zhang & Yeung, 2010; Jawanpuria & Nath, 2011; Ciliberto et al., 2015). However, those works require singular value decomposition (SVD) of \mathbf{W} matrix at every iteration, which is computationally costly for large-scale applications. In the following lemma, we analyze a dual formulation of (3) that is suitable for learning large-scale structured matrix learning. The dual formulation gives further insights into the optimization problem (3) and its optimal solution.

Lemma 2. Let l_{ti}^* be the Fenchel conjugate function of the loss: $l_{ti} : \mathbb{R} \rightarrow \mathbb{R}$, $v \mapsto l(y_{ti}, v)$. The dual problem of (3) with respect to \mathbf{W} is

$$\min_{\Theta \in \mathcal{P}^d} g(\Theta), \quad (4)$$

where $g : \mathcal{P}^d \rightarrow \mathbb{R} : \Theta \mapsto g(\Theta)$ is the following convex function

$$g(\Theta) := \max_{s \in \mathbb{R}^n} \sum_{t=1}^T \left(\max_{z_t \in \mathbb{R}^d} -C \sum_{i=1}^d l_{ti}^* \left(\frac{-z_{ti}}{C} \right) - \frac{1}{2} (z_t + a_t)^\top \Theta (z_t + a_t) \right), \quad (5)$$

$[a_1, \dots, a_T] = \mathcal{A}^*(s)$ and $\mathcal{A}^* : \mathbb{R}^n \rightarrow \mathbb{R}^{d \times T}$ is the adjoint of \mathcal{A} . Furthermore, let Θ^* be an optimal solution of (4) and $\{s^*, (z_t^*)_{t=1}^T\}$ be corresponding optimal solution of (5), then the optimal solution $\mathbf{W}^* := [w_1^*, \dots, w_T^*]$ of (3) is given by $w_t^* = \Theta^*(z_t^* + a_t^*)$, where $[a_1^*, \dots, a_T^*] = \mathcal{A}^*(s^*)$.

Optimization over \mathbf{U}

$$\min_{\mathbf{U} \in \mathcal{S}_r^d} \max_{s \in \mathbb{R}^n, z_t \in \mathbb{R}^d \forall t} \sum_{t=1}^T \left(-C \sum_{i=1}^d l_{ti}^* \left(\frac{-z_{ti}}{C} \right) - \frac{1}{2} (z_t + a_t)^\top \mathbf{U} \mathbf{U}^\top (z_t + a_t) \right)$$

Application specific algorithm

Figure 1: Proposed algorithmic framework for structured low-rank matrix learning. Low-rank constraint is enforced via \mathbf{U} and application specific structural constraints are enforced via $\{s, (z_t)_{t=1}^T\}$.

Lemma 2 has several implications. First, the optimal w_t^* is a product of two terms, Θ^* and $z_t^* + a_t^*$. The low-rank constraint is enforced through Θ^* and the structural constraint is enforced through $z_t^* + a_t^*$. This facilitates using simpler optimization techniques as compared to the case where both the constraints are enforced on a single variable. In applications where the constraint $\mathcal{A}(\mathbf{W}) = \mathbf{0}$ is absent, the problem (5) can be solved in parallel across t . It should be noted that the dual formulation (5) is smooth (with bounded constraints on the dual variables z) even for non-smooth loss functions such as the ℓ_1 -loss and ϵ -SVR loss.

Existing multi-task algorithms that tackle saddle point optimization problems of the form (4) require a projection operation onto \mathcal{P}^d every iteration (Zhang & Yeung, 2010; Jawanpuria & Nath, 2011). The projection operation is accomplished using an eigenvalue decomposition, which costs $O(d^3)$. This is prohibitive in a large-scale setup. To this end, we explicitly constrain the rank of Θ in (4) in the next section.

3 Novel Formulation via Fixed-rank Parameterization of Θ

We model $\Theta \in \mathcal{P}^d$ as a rank r matrix as follows: $\Theta = \mathbf{U} \mathbf{U}^\top$, where $\mathbf{U} \in \mathbb{R}^{d \times r}$ and $\|\mathbf{U}\|_F = 1$. The proposed modeling has several benefits in large scale low-rank matrix learning problems, where $r \ll \min\{d, T\}$ is a common setting. *First*, the parameterization ensures that $\Theta \in \mathcal{P}^d$ constraint is always satisfied. This saves the costly projection operations to ensure $\Theta \in \mathcal{P}^d$. Enforcing $\|\mathbf{U}\|_F = 1$ constraint costs $O(rd)$. *Second*, the dimension of the search space of problem (4) with $\Theta = \mathbf{U} \mathbf{U}^\top$ is $rd - 1 - r(r-1)/2$ (Journée et al., 2010), which is much lower than the dimension $(d(d+1)/2 - 1)$ of $\Theta \in \mathcal{P}^d$. By restricting the search space for Θ , we gain computational efficiency. *Third*, increasing the parameter C in (4) and (3) promotes low training error but high rank of the solution, and vice-versa. The proposed fixed-rank parameterization decouples this trade-off.

We re-write (4) and (5) in terms of the proposed parameterization $\Theta = \mathbf{U} \mathbf{U}^\top$ as follows:

$$\min_{\mathbf{U} \in \mathbb{R}^{d \times r}, \|\mathbf{U}\|_F = 1} g(\mathbf{U} \mathbf{U}^\top), \text{ where} \tag{6}$$

$$g(\mathbf{U} \mathbf{U}^\top) := \max_{s \in \mathbb{R}^n} \sum_{t=1}^T \max_{z_t \in \mathbb{R}^d} \left(-C \sum_{i=1}^d l_{ti}^* \left(\frac{-z_{ti}}{C} \right) - \frac{1}{2} \left\| \mathbf{U}^\top (z_t + a_t) \right\|_F^2 \right). \tag{7}$$

Figure 1 presents the overall design of our framework. The outer (global) minimization problem over \mathbf{U} aims to learn optimal low-dimensional latent space for \mathbf{W} , and the inner (local) maximization problem over $\{s, (z_t)_{t=1}^T\}$ learns the best \mathbf{W} in that space that satisfy the structural constraints $\mathcal{A}(\mathbf{W}) = \mathbf{0}$. We emphasize that though (6) is a non-convex problem in \mathbf{U} , the optimization problem in (7) is convex in $\{s, (z_t)_{t=1}^T\}$ for a given \mathbf{U} . The specialized formulations of $g(\mathbf{U} \mathbf{U}^\top)$ in (7) for several applications are presented next.

Table 1: Specialized expression of $g(\mathbf{U}\mathbf{U}^\top)$ for various structured low-rank matrix learning problems.

Problem	$g(\mathbf{U}\mathbf{U}^\top)$ as defined in (7)	Algorithm for solving (7)
Hankel Matrix Learning (square loss)	$\max_{s_t \in \mathbb{R}^d, z_t \in \mathbb{R}^{d+T-1}} \langle y_t, z_t \rangle - \frac{1}{4C} \langle z_t, z_t \rangle - \frac{1}{2} \sum_{t=1}^T \langle \mathbf{U}^\top s_t, \mathbf{U}^\top s_t \rangle$ subject to $:z_k - \sum_{\substack{(i,t): i+t=k, \\ 1 \leq i \leq d, 1 \leq t \leq T}} s_{ti} = 0 \quad \forall k = 2, \dots, d+T$	Preconditioned [#] conjugate gradients (Barrett et al., 1994)
Matrix [‡] Completion (square loss)	$\sum_{t=1}^T \max_{z_t} \langle y_t, z_t \rangle - \frac{1}{4C} \langle z_t, z_t \rangle - \frac{1}{2} \langle \mathbf{U}_{\Omega_t}^\top z_t, \mathbf{U}_{\Omega_t}^\top z_t \rangle$	Least square solver [§]
Robust [‡] Matrix Completion (ℓ_1 -loss)	$\sum_{t=1}^T \max_{z_t \in [-C, C]^{m_t}} \langle y_t, z_t \rangle - \frac{1}{2} \langle \mathbf{U}_{\Omega_t}^\top z_t, \mathbf{U}_{\Omega_t}^\top z_t \rangle$	Dual coordinate descent [§] (Ho & Lin, 2012)
Multi-task [‡] Feature Learning (square loss)	$\sum_{t=1}^T \max_{z_t} \langle y_t, z_t \rangle - \frac{1}{4C} \langle z_t, z_t \rangle - \frac{1}{2} \langle \mathbf{U}^\top \mathbf{X}_t z_t, \mathbf{U}^\top \mathbf{X}_t z_t \rangle$	Least square solver [§]

[#] The equality constraints are handled efficiently by using an affine projection operator.
[§] Problem for each t can be solved in parallel.
[‡] $\mathbf{U}_{\Omega_t} \in \mathbb{R}^{m_t \times r}$ represents only those rows of \mathbf{U} whose corresponding indices are observed in the t^{th} column of \mathbf{Y} .

Specialized Formulations for Various Problems

Table 1 lists the expressions of $g(\mathbf{U}\mathbf{U}^\top)$ and the corresponding algorithms for computing them in the following applications. a) **Hankel matrix learning:** Hankel matrices have the structural constraint that its anti-diagonal entries are same. Given a vector $y = [y_1, y_2, \dots, y_7]$, a Hankel matrix corresponding to it is

$$\begin{bmatrix} y_1 & y_2 & y_3 & y_4 & y_5 \\ y_2 & y_3 & y_4 & y_5 & y_6 \\ y_3 & y_4 & y_5 & y_6 & y_7 \end{bmatrix}.$$

In certain linear time-invariant systems and stochastic system realization problems, learning a low-rank Hankel matrix corresponding to a given vector y is equivalent to finding a low-order linear model for the data (Fazel et al., 2013; Markovsky & Usevich, 2013; Markovsky, 2014), b) **Matrix completion:** Given a partially observed matrix \mathbf{Y} at indices Ω , we learn the full matrix \mathbf{W} (Toh & Yun, 2010; Cai et al., 2010), c) **Robust matrix completion:** Matrix completion with robust loss function such as the ℓ_1 -loss or ϵ -SVR loss (Candès & Plan, 2009; Cambier & Absil, 2016), and d) **Multi-task feature learning:** The aim here is to learn a low-dimensional latent feature representation common across all the given tasks (Argyriou et al., 2008; Jawanpuria & Nath, 2011). Each task t is a regression/classification problem with the training data set $\{\mathbf{X}_t, y_t\}$.

In the next section, we present our optimization algorithm for problem (6).

4 Proposed Optimization on Spectrahedron Manifold

The matrix \mathbf{U} lies in, what is popularly known as, the *spectrahedron* manifold $\mathcal{S}_r^d := \{\mathbf{U} \in \mathbb{R}^{d \times r} : \|\mathbf{U}\|_F = 1\}$. Specifically, the spectrahedron manifold has the structure of a Riemannian quotient manifold (Journée et al., 2010). The quotient structure takes the rotational invariance of the constraint $\|\mathbf{U}\|_F = 1$ into account. It should be noted that the Riemannian view of (6) is conceptually different from the Euclidean view: the former embeds the constraint $\mathbf{U} \in \mathcal{S}_r^d$ into the search space. Hence, the Riemannian manifold optimization framework translates the constrained optimization problem (6) into an *unconstrained* optimization problem over the nonlinear manifold \mathcal{S}_r^d . The conventional (Euclidean) first- (*e.g.*, steepest descent and conjugate gradients) and second-order (trust regions) algorithms have their Riemannian manifold counterparts with similar convergence guarantees (Absil et al., 2008; Journée et al., 2010; Sato & Iwai, 2013). The particular details are provided in the supplementary material.

Algorithm 1 Proposed first- and second-order algorithms for (6)

Input: $\{y_t\}_{t=1}^T$, rank r , regularization parameter C .

Initialize $\mathbf{U} \in \mathcal{S}_r^d$.

repeat

1: Solve for $\{s, (z_t)_{t=1}^T\}$ by computing $g(\mathbf{U}\mathbf{U}^\top)$ as in (7).

2: Compute $\nabla_{\mathbf{U}}g(\mathbf{U}\mathbf{U}^\top)$ as given in Lemma 3.

3: **Riemannian CG step:** compute a conjugate direction \mathbf{V} and step size α using Armijo line search. It makes use of $\nabla_{\mathbf{U}}g(\mathbf{U}\mathbf{U}^\top)$.

3: **Riemannian TR step:** compute a search direction \mathbf{V} which minimizes the trust region sub-problem. It makes use of $\nabla_{\mathbf{U}}g(\mathbf{U}\mathbf{U}^\top)$ and its directional derivative. Step size $\alpha = 1$.

4: Update $\mathbf{U} = (\mathbf{U} + \alpha\mathbf{V})/\|\mathbf{U} + \alpha\mathbf{V}\|_F$ (retraction step)

until convergence

Output: $\{\mathbf{U}, s, (z_t)_{t=1}^T\}$ and $\mathbf{W} = \mathbf{U}\mathbf{U}^\top([z_1, \dots, z_T] + \mathcal{A}^*(s))$.

Our framework readily allows to propose Riemannian conjugate gradient (CG) and trust-region (TR) algorithms for (6). These require the notions of the *Riemannian gradient* (first-order derivative of the objective function on the manifold), *Riemannian Hessian* along a search direction (the *covariant* derivative of the Riemannian gradient along a tangential direction on the manifold), and the *retraction* operator (that ensures that we always stay on the manifold). The Riemannian gradient and Hessian notions require computations of the standard (Euclidean) gradient and the directional derivative of this gradient along a given search direction (6), which are expressed in the following lemma.

Lemma 3. Let $\{\hat{s}, (\hat{z}_t)_{t=1}^T\}$ be an optimal solution of the convex problem (7) at \mathbf{U} and $[\hat{a}_1, \dots, \hat{a}_T] = \mathcal{A}^*(\hat{s})$. Let $\nabla_{\mathbf{U}}g(\mathbf{U}\mathbf{U}^\top)$ denote the gradient of $g(\mathbf{U}\mathbf{U}^\top)$ at \mathbf{U} and $D\nabla_{\mathbf{U}}g(\mathbf{U}\mathbf{U}^\top)[\mathbf{V}]$ denote the directional derivative of the gradient $\nabla_{\mathbf{U}}g(\mathbf{U}\mathbf{U}^\top)$ along $\mathbf{V} \in \mathbb{R}^{d \times r}$. Let $\{\dot{s}, (\dot{z}_t)_{t=1}^T\}$ denote the directional derivative of $\{s, (z_t)_{t=1}^T\}$ along \mathbf{V} at $\{\hat{s}, (\hat{z}_t)_{t=1}^T\}$ and $[\dot{a}_1, \dots, \dot{a}_T] = \mathcal{A}^*(\dot{s})$. Then,

$$\begin{aligned} \nabla_{\mathbf{U}}g(\mathbf{U}\mathbf{U}^\top) &= -\left(\sum_{t=1}^T (\hat{z}_t + \hat{a}_t)(\hat{z}_t + \hat{a}_t)^\top\right)\mathbf{U} \\ D\nabla_{\mathbf{U}}g(\mathbf{U}\mathbf{U}^\top)[\mathbf{V}] &= -\sum_{t=1}^T \left((\hat{z}_t + \hat{a}_t)(\hat{z}_t + \hat{a}_t)^\top\mathbf{V} + (\dot{z}_t + \dot{a}_t)(\hat{z}_t + \hat{a}_t)^\top\mathbf{U} + (\hat{z}_t + \hat{a}_t)(\dot{z}_t + \dot{a}_t)^\top\mathbf{U}\right). \end{aligned}$$

It can be observed from Lemma 3 that the gradient $\nabla_{\mathbf{U}}g(\mathbf{U}\mathbf{U}^\top)$ depends on the optimal solution of the convex problem (7). Table 1) contains the exact solvers for solving (7) in specific applications. For example, in matrix completion and multi-task feature learning problems, (7) can be solved in closed form.

Algorithm 1 summarizes the proposed first- and second-order algorithms for solving (6). Our first-order algorithm computes the Riemannian *conjugate* gradient direction. We perform *Armijo* line search on \mathcal{S}_r^d to compute a step-size that sufficiently decreases $g(\mathbf{U}\mathbf{U}^\top)$ on the manifold. We update along the conjugate direction with the step-size by *retraction*. Our second-order algorithm (Algorithm 1) solves a Riemannian trust-region *sub-problem* (in a neighborhood) at every iteration. Solving the trust-region sub-problem leads to a search direction that minimizes a *quadratic* model of $g(\mathbf{U}\mathbf{U}^\top)$ on the manifold. Solving this sub-problem does not require inverting the full Hessian of the objective function. We employ iterative algorithms (Absil et al., 2008, Chapter 7) that make use of the directional derivative of the gradient, $D\nabla_{\mathbf{U}}g(\mathbf{U}\mathbf{U}^\top)[\mathbf{V}]$ (as computed in Lemma 3). Algorithm 1 terminates when $\|\nabla_{\mathbf{U}}g(\mathbf{U}\mathbf{U}^\top)\|_F \leq \epsilon$, where ϵ is a pre-defined tolerance threshold. In large-scale experiments, we follow the common practice of also having an upper limit on the number of iterations (Toh & Yun, 2010; Hsieh & Olsen, 2014; Cambier & Absil, 2016; Wen et al., 2012; Mishra & Sepulchre, 2014; Yu et al., 2014; Boumal & Absil, 2015; Tan et al., 2016). Although we have focused on CG and TR algorithms for (6) in this paper, our approach can be readily extended to a stochastic setting, e.g., when columns are streamed one by one.

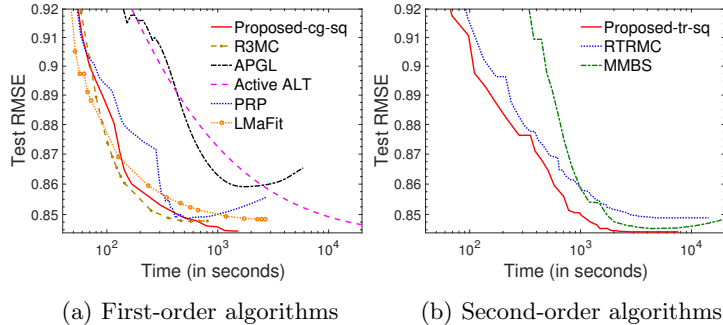


Figure 2: Evolution of test RMSE on the Netflix data set

Table 2: Test RMSE on matrix completion.

	NetfliX	ML10m	ML20m
Proposed-tr-sq	0.8443	0.8026	0.7962
Proposed-cg-sq	0.8449	0.8026	0.7963
R3MC	0.8478	0.8070	0.7982
RTRMC	0.8489	0.8161	0.8044
APGL	0.8587	0.8283	0.8160
Active ALT	0.8463	0.8116	0.8033
MMBS	0.8454	0.8226	0.8053
LMaFit	0.8484	0.8082	0.7996
PRP	0.8488	0.8068	0.7987

5 Experiments

In this section, we evaluate the generalization performance as well as computational efficiency of our approach against state-of-the-art in four different applications — matrix completion, robust matrix completion, Hankel matrix learning, and multi-task learning. All our algorithms are implemented using the Manopt toolbox (Boumal et al., 2014). Implementation and parameter tuning details, data set statistics, and additional results are provided in the supplementary material.

5.1 Matrix Completion

Our first- and second-order methods (Algorithm 1) with square loss are denoted by Proposed-cg-sq and Proposed-tr-sq, respectively.

Baseline techniques: We compare against state-of-the-art fixed-rank and nuclear norm minimization based matrix completion solvers: APGL: accelerated proximal gradient algorithm for nuclear norm minimization (Toh & Yun, 2010), Active ALT: first-order nuclear norm solver based on active subspace selection (Hsieh & Olsen, 2014), R3MC: fixed-rank Riemannian preconditioned non-linear conjugate gradient algorithm (Mishra & Sepulchre, 2014), LMaFit: nonlinear successive over-relaxation algorithm based on alternate least squares (Wen et al., 2012), MMBS: fixed-rank second-order nuclear norm minimization algorithm (Mishra et al., 2013). RTRMC: fixed-rank second-order Riemannian preconditioned algorithm on the Grassmann manifold (Boumal & Absil, 2011, 2015), and PRP: a recent proximal Riemannian pursuit algorithm Tan et al. (2016).

Parameter settings: The regularization parameters for respective algorithms are cross-validated to obtain their best generalization performance. The initialization for all the algorithms is based on the first few singular vectors of the given partially complete matrix \mathbf{Y} (Boumal & Absil, 2015). All the fixed algorithms (R3MC, LMaFit, MMBS, RTRMC, Proposed-cg-sq, Proposed-tr-sq) are provided the rank $r = 10$. In all variable rank approaches (APGL, Active ALT, PRP), the maximum rank parameter is set to 10. We run all the methods on ten random 80/20 train/test splits.

Results: Figures 2 (a)&(b) display the evolution of root mean squared error on the test set (test RMSE) against the training time on the Netflix data set (Recht & Ré, 2013) for first- and second-order algorithms, respectively. Proposed-cg-sq is among the most efficient first-order method and Proposed-tr-sq is the best second-order method. We outperform both APGL and Active ALT, and both our algorithms converge to a lower test RMSE than MMBS at a much faster rate. Table 2 reports the minimum test RMSE, averaged over ten splits, obtained by all the algorithms on three large-scale real-world data sets: Netflix, MovieLens10m (ML10m), and MovieLens20m (ML20m) (MovieLens, 1997). Both our algorithms obtain the smallest test RMSE.

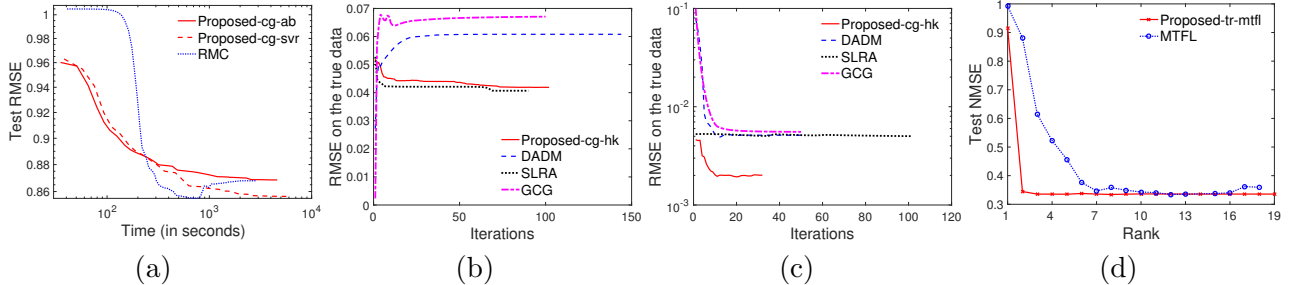


Figure 3: (a) Evolution of test RMSE of different robust matrix completion algorithms on the Netflix data set; (b) & (c) Performance on different stochastic system realization problems, learning low-rank Hankel matrices; (d) Generalization performance vs rank on multi-task feature learning problem.

5.2 Robust Matrix Completion

We compare the following robust matrix completion algorithms: RMC (Cambier & Absil, 2016): state-of-the-art first-order Riemannian optimization algorithm that employs the smooth pseudo-Huber loss function (which successively approximates absolute loss), Proposed-cg-ab: our first-order algorithm with ℓ_1 -loss, and Proposed-cg-svr: our first-order algorithm employing ϵ -SVR loss. It should be emphasized that the non-smooth nature of ℓ_1 -loss and ϵ -SVR loss makes them challenging to optimize in large-scale low-rank settings. All the three loss functions are known to be robust to noise. We follow the same experimental setup described in the previous section.

Figure 3(a) show the results on the Netflix data set. We observe that both our algorithms scale effortlessly on the Netflix data set, with Proposed-cg-svr obtaining the best generalization result. It should be noted RMC approximates ℓ_1 -loss only towards to the end of its iterations. The test RMSE obtained at convergence are: 0.8685 (Proposed-cg-ab), **0.8565** (Proposed-cg-svr), and 0.8678 (RMC), respectively.

5.3 Stochastic system realization (SSR)

Given the observation of noisy system output, the goal in SSR problem is to find a minimal order autoregressive moving-average model (Fazel et al., 2013; Yu et al., 2014). The order of such a model can be shown to be equal to the rank of the Hankel matrix consisting of the exact process covariances (Fazel et al., 2013; Yu et al., 2014). Hence, finding a low-order model is equivalent to learning a low-rank Hankel matrix, while being close to the given data. We perform a small and a large-scale experiment in this problem setup.

In our first experiment experiment, the data is generated in accordance with the setting detailed in Fazel et al. (2013); Yu et al. (2014), with $d = 21$, $T = 100$, and $r = 10$. We compare our first-order low-rank Hankel matrix learning algorithm, Proposed-cg-hk, with state-of-the-art solvers GCG (Yu et al., 2014), SLRA (Markovsky, 2014; Markovsky & Usevich, 2014), and DADM (Fazel et al., 2013). We learn a rank-10 Hankel matrix with all the algorithms. Since GCG and DADM have a nuclear norm regularization, we tune their regularization parameter to vary the rank. Proposed-cg-hk is initialized with a random \mathbf{U} matrix, SLRA employ SVD based initialization provided by its authors, and GCG and DADM are initialized with the input training matrix. It should be noted that both DADM and GCG are convex approaches and their converged solutions are independent of the initialization. The best result with rank less than or equal to 10 has been reported for GCG and DADM. Figure 3(b) plots the variation of RMSE with respect to true data (true RMSE) across iterations. It should be noted that the training data is a noisy version of true data. We observe

that our algorithm outperforms GCG and DADM and matches SLRA in terms of generalization performance. The true RMSE at convergence is: 0.0419 (Proposed-cg-hk), 0.0671 (GCG), 0.0608 (DADM) and **0.0407** (SLRA). In our second experiment, we generated the data in accordance with the setting detailed in (Markovsky, 2014; Markovsky & Usevich, 2014). We set $d = 1000$, $T = 10000$, and $r = 5$ and repeat the above experiment. The true RMSE is plotted in Figure 3(c). We observe that our algorithm gives lowest true RMSE.

5.4 Multi-task Learning

In this experiment, we compare the generalization performance of our multi-task feature learning algorithm Proposed-tr-mtfl (for the formulation in Table 1, row 4) with the convex multi-task feature learning algorithm MTFL (Argyriou et al., 2006, 2008). It should be stated that MTFL solves the convex formulation 3 without the $\mathcal{A}(\mathbf{W}) = \mathbf{0}$ constraint optimally via an alternate optimization algorithm. Optimal solution for MTFL at different ranks is obtained by tracing the solution path with respect to parameter C , whose value is varied as $\{2^{-8}, 2^{-7}, \dots, 2^{24}\}$. We vary the rank parameter r in our algorithm to obtain different ranked solutions for a given C . The experiments are performed on two benchmark multi-task regression data sets: a) Parkinsons: we need to predict the Parkinson’s disease symptom score of 42 patients (Frank & Asuncion, 2010); b) School: we need to predict performance of all students in 139 schools. Following (Argyriou et al., 2008; Zhang & Yeung, 2010), we report the normalized mean square error over the test set (test NMSE). Figures 3(d) present the results on the Parkinsons data set. We observe from the figure that our method achieves the better generalization performance at low ranks compared to MTFL. Similar results are obtained on the School data set (details are in supplementary).

6 From Local Solution of (6) to Global Solution of (4)

Experiments discussed in Section 5 show that the proposed rank-constrained formulation for structured low-rank matrix learning (6) obtains state-of-the-art performance across several applications. Since the formulation (6) is motivated from the convex formulation (4), it is natural to ask the question: “*when can a locally optimal solution of (6) results in the globally optimal solution of (4)?*”. In this section, we give a practically verifiable answer. We begin with the following lemma that provides a characterization of an optimal solution of (4). It is a special case of the general result proved by (Journée et al., 2010, Theorem 7 and Corollary 8).

Lemma 4. *Let \mathbf{U}^* be a local minimizer of the non-convex problem (6). If $\text{rank}(\mathbf{U}^*) < r$ or $r = d$, then $\Theta^* = \mathbf{U}^*(\mathbf{U}^*)^\top$ is a stationary point for the convex problem (4).*

Consequently, given a local minimizer \mathbf{U}^* of (6), we can verify whether the candidate solution $\Theta = \mathbf{U}^*(\mathbf{U}^*)^\top$ is optimal for (4) by simply computing the minimum singular value of \mathbf{U}^* . Our next result presents a stronger optimality characterization through a duality gap criterion for (4) with respect to any *feasible* solution $\hat{\mathbf{U}}$ of (6).

Proposition 1. *Let $\hat{\mathbf{U}}$ be a feasible solution of (6). Then, a candidate solution for (4) is $\hat{\Theta} = \hat{\mathbf{U}}\hat{\mathbf{U}}^\top$. Let $\{\hat{s}, (\hat{z}_t)_{t=1}^T\}$ be an optimal solution of the convex problem in (7) at $\hat{\mathbf{U}}$. In addition, let σ_1 be the maximum singular of the the matrix whose t^{th} column is $(\hat{z}_t + \hat{a}_t)$, where $[\hat{a}_1, \dots, \hat{a}_T] = \mathcal{A}^*(\hat{s})$. The duality gap (Δ) associated with $\{\hat{\Theta}, \hat{s}, (\hat{z}_t)_{t=1}^T\}$ for (4) is given by $\Delta = \frac{1}{2}(\sigma_1^2 - \sum_{t=1}^T \|\hat{\mathbf{U}}^\top(\hat{z}_t + \hat{a}_t)\|^2)$.*

It should be stated that computing σ_1 in Proposition 1 is computationally cheap (e.g., with few *power iteration* updates).

The above results show that if we vary the rank r from low to high and run the proposed Algorithm 1, we eventually converge to the globally optimal solution of (4) and obtain the duality gap close to zero. This is indeed observed in Figure 4(a). The result is obtained from our multi-

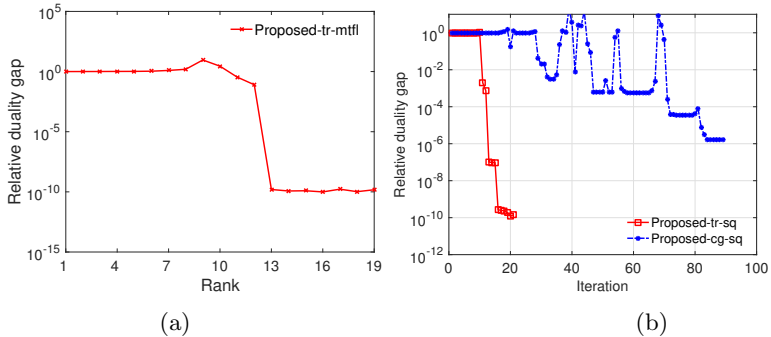


Figure 4: (a) Relative duality gap vs rank, (b) Relative duality gap vs iterations.

task feature learning algorithm Proposed-tr-mtfl (for the formulation in Table 1, row 4) on the benchmark Parkinsons multi-task regression data set (Frank & Asuncion, 2010). Figure 4(a) shows that we attain a very small relative duality gap when rank $r \geq 13$, which is less than $d = 19$.

Figure 4(b) plots the relative duality gap for the proposed first- and second-order algorithms (Algorithm 1) for a synthetic matrix completion problem instance. The data set is generated following the procedure detailed by (Boumal & Absil, 2015) for a rank-5 matrix with $d = 5000$, $T = 500000$, and the number of observed entries for training being 15 149 850. We observe that both our algorithms converge towards the global optimum of (4).

7 Conclusion

We present a generic framework for learning low-rank matrices with structural constraints. The structured low-rank matrix learning problem is modeled as a novel rank-constrained saddle point optimization problem. The benefit of this modeling is that it decouples the low-rank and structural constraints onto separate factors. The optimization problem is shown to lie on the Riemannian spectrahedron manifold. The Riemannian structure enables to propose computationally efficient conjugate gradient and trust-region algorithms for structured low-rank matrix learning. Our algorithms scale readily to the Netflix data set even with non-smooth loss functions such as the ℓ_1 -loss and ϵ -SVR loss. We obtain state-of-the-art generalization performance on standard and robust matrix completion, low-rank Hankel matrix learning, and multi-task feature learning problems. We additionally provide a practical way of characterizing how far our local solution is to the global minimum of a convex program.

Acknowledgement

We thank Léopold Cambier, Ivan Markovskiy, and Konstantin Usevich for useful discussions on the work. We thank Adams Wei Yu and Mingkui Tan for making their codes available.

References

- Absil, P.-A., Mahony, R., and Sepulchre, R. *Optimization Algorithms on Matrix Manifolds*. Princeton University Press, Princeton, NJ, 2008.
- Amit, Y., Fink, M., Srebro, N., and Ullman, S. Uncovering shared structures in multiclass classification. In *International Conference on Machine Learning (ICML)*, pp. 17–24, 2007.

- Argyriou, A., Evgeniou, T., and Pontil, M. Multi-task feature learning. In *Neural Information Processing Systems conference (NIPS)*, 2006.
- Argyriou, A., Evgeniou, T., and Pontil, M. Convex multi-task feature learning. *Machine Learning*, 73:243–272, 2008.
- Barrett, R., Berry, M., Chan, T. F., Demmel, J., Donato, J., Dongarra, J., Eijkhout, V., Pozo, R., Romine, C., and der Vorst, H. Van. *Templates for the Solution of Linear Systems: Building Blocks for Iterative Methods, 2nd Edition*. SIAM, 1994.
- Bertsekas, D. *Nonlinear Programming*. Athena Scientific, 1999. URL <http://www.athenasc.com/nonlinbook.html>.
- Bhaskar, S. A. and Javanmard, A. 1-bit matrix completion under exact low-rank constraint. In *Annual Conference on Information Sciences and Systems (CISS)*, pp. 1–6, 2015.
- Bonnans, J. F. and Shapiro, A. *Perturbation Analysis of Optimization Problems*. Springer-Verlag, 2000.
- Boumal, N. and Absil, P.-A. RTRMC: A Riemannian trust-region method for low-rank matrix completion. In *Advances in Neural Information Processing Systems 24 (NIPS)*, pp. 406–414, 2011.
- Boumal, N. and Absil, P.-A. Low-rank matrix completion via preconditioned optimization on the Grassmann manifold. *Linear Algebra and its Applications*, 475:200–239, 2015.
- Boumal, N., Mishra, B., Absil, P.-A., and Sepulchre, R. Manopt: a Matlab toolbox for optimization on manifolds. *Journal of Machine Learning Research*, 15(Apr):1455–1459, 2014.
- Box, G. E. P. and Jenkins, G. *Time Series Analysis, Forecasting and Control*. Holden-Day, Incorporated, 1990.
- Boyd, S. and Vandenberghe, L. *Convex Optimization*. Cambridge University Press, 2004. URL <http://www.stanford.edu/~boyd/cvxbook/>.
- Cai, J. F., Candès, E. J., and Shen, Z. A singular value thresholding algorithm for matrix completion. *SIAM Journal on Optimization*, 20(4):1956–1982, 2010.
- Cambier, L. and Absil, P. A. Robust low-rank matrix completion by Riemannian optimization. *SIAM J. Sci. Comput.*, 38(5):S440—S460, 2016.
- Candès, E. J. and Plan, Y. Matrix completion with noise. *Proceedings of the IEEE*, 98(6):925–936, 2009.
- Candès, E. J. and Recht, B. Exact matrix completion via convex optimization. *Foundations of Computational Mathematics*, 9(6):717–772, 2009.
- Ciliberto, C., Mroueh, Y., Poggio, T., and Rosasco, L. Convex learning of multiple tasks and their structure. In *International Conference on Machine Learning (ICML)*, 2015.
- Davenport, M. A., Plan, Y., van den Berg, E., and Wooters, M. 1-bit matrix completion. *Information and Inference*, 3(3):189–223, 2014.

- Fazel, M., Kei, P. T., Sun, D., and Tseng, P. Hankel matrix rank minimization with applications to system identification and realization. *SIAM Journal on Matrix Analysis and Applications*, 34(3):946–977, 2013.
- Frank, A. and Asuncion, A. UCI machine learning repository, 2010. URL <http://archive.ics.uci.edu/ml>.
- Ho, C. H. and Lin, C. J. Large-scale linear support vector regression. *Journal of Machine Learning Research*, 13(1):3323–3348, 2012.
- Hsieh, C.-J. and Olsen, P. A. Nuclear norm minimization via active subspace selection. In *International Conference on Machine learning (ICML)*, 2014.
- Jawanpuria, P. and Nath, J. S. Multi-task multiple kernel learning. In *SIAM International Conference on Data Mining (SDM)*, pp. 828–83, 2011.
- Journée, M., Bach, F., Absil, P.-A., and Sepulchre, R. Low-rank optimization on the cone of positive semidefinite matrices. *SIAM Journal on Optimization*, 20(5):2327–2351, 2010.
- Kannan, R., Ishteva, M., and Park, P. Bounded matrix factorization for recommender system. *Knowledge and information systems*, 39(3):491–511, 2014.
- Marecek, J., Richtarik, P., and Takac, M. Matrix completion under interval uncertainty. *European Journal of Operational Research*, 256(1):35–43, 2017.
- Markovsky, I. Recent progress on variable projection methods for structured low-rank approximation. *Signal Processing*, 96(Part B):406–419, 2014.
- Markovsky, I. and Usevich, K. Structured low-rank approximation with missing data. *SIAM Journal on Matrix Analysis and Applications*, 34(2):814–830, 2013.
- Markovsky, I. and Usevich, K. Software for weighted structured low-rank approximation. *J. Comput. Appl. Math.*, 256:278–292, 2014.
- Mishra, B. and Sepulchre, R. R3MC: A Riemannian three-factor algorithm for low-rank matrix completion. In *Proceedings of the 53rd IEEE Conference on Decision and Control (CDC)*, pp. 1137–1142, 2014.
- Mishra, B., Meyer, G., Bach, F., and Sepulchre, R. Low-rank optimization with trace norm penalty. *SIAM Journal on Optimization*, 23(4):2124–2149, 2013.
- MovieLens. MovieLens, 1997. URL <http://grouplens.org/datasets/movielens/>.
- Recht, B. and Ré, C. Parallel stochastic gradient algorithms for large-scale matrix completion. *Mathematical Programming Computation*, 5(2):201–226, 2013.
- Sato, H. and Iwai, T. A new, globally convergent Riemannian conjugate gradient method. *Optimization: A Journal of Mathematical Programming and Operations Research*, 64(4):1011–1031, 2013.
- Sion, M. On General Minimax Theorem. *Pacific Journal of Mathematics*, 1958.
- Tan, M., Xiao, S., Gao, J., Xu, D., van den Hengel, A., and Shi, Q. Proximal riemannian pursuit for large-scale trace-norm minimization. In *The IEEE Conference on Computer Vision and Pattern Recognition (CVPR)*, 2016.

- Toh, K. C. and Yun, S. An accelerated proximal gradient algorithm for nuclear norm regularized least squares problems. *Pacific Journal of Optimization*, 6(3):615–640, 2010.
- Vandereycken, B. Low-rank matrix completion by Riemannian optimization. *SIAM Journal on Optimization*, 23(2):1214–1236, 2013.
- Wen, Z., Yin, W., and Zhang, Y. Solving a low-rank factorization model for matrix completion by a nonlinear successive over-relaxation algorithm. *Mathematical Programming Computation*, 4(4): 333–361, 2012.
- Wright, J., Ganesh, A., Rao, S., Peng, Y., and Ma, Y. Robust principal component analysis: Exact recovery of corrupted low-rank matrices via convex optimization. In *Neural Information Processing Systems conference (NIPS)*, 2009.
- Yu, A. W., W., Ma, Y., Yu, G., Carbonell J., and S., Sra. Efficient structured matrix rank minimization. In *Advances in Neural Information Processing Systems (NIPS)*, 2014.
- Yuan, M., Ekici, A., Lu, Z., and Monteiro, R.D.C. Dimension reduction and coefficient estimation in multivariate linear regression. *Journal of the Royal Statistical Society: Series B (Statistical Methodology)*, 69(3):329–346, 2007.
- Zhang, Y. and Yeung, D. Y. A convex formulation for learning task relationships in multi-task learning. In *Uncertainty in Artificial Intelligence*, 2010.

Supplementary material

Abstract

This is the supplementary material to the main paper titled ‘A Saddle Point Approach to Structured Low-rank Matrix Learning’. Section A.1 contains the proof of Lemma 2 proposed in the main paper. Section A.2 contains the proof of Lemma 3 proposed in the main paper. Section A.3 contains the proof of Proposition 1 proposed in the main paper. Section A.4 briefly describes the Riemannian optimization framework employed in our algorithms discussed in Section 3 of the main paper. Section A.5 presents the complete experimental results and related details. The sections, equations, tables, figures and algorithms from the main paper are referred in their original numbers. The sections, equations, tables and figures introduced in this supplementary have the numbering scheme of the form ‘A.x’.

A.1 Lemma 2 and its Proof

Lemma 2 gives the dual problem of the following primal problem with respect to variable \mathbf{W} :

$$\min_{\Theta \in \mathcal{P}^d} \sum_{t=1}^T \min_{w_t \in \mathbb{R}^d} \frac{1}{2} w_t^\top \Theta^\dagger w_t + C \sum_{i=1}^d l(y_{ti}, w_{ti}) \quad (\text{A.1})$$

subject to $w_t \in \text{range}(\Theta), \forall t = 1, \dots, T$ and $\mathcal{A}(\mathbf{W}) = \mathbf{0}$, where $\text{range}(\Theta) = \{\Theta z : z \in \mathbb{R}^d\}$. In the following, we restate Lemma 2 from the main paper (for convenience) and prove it.

Lemma 2. *Let l_{ti}^* be the Fenchel conjugate function of the loss: $l_{ti} : \mathbb{R} \rightarrow \mathbb{R}, v \mapsto l(y_{ti}, v)$. The dual of (A.1) with respect to \mathbf{W} is*

$$\min_{\Theta \in \mathcal{P}^d} g(\Theta), \quad (\text{A.2})$$

where $g : \mathcal{P}^d \rightarrow \mathbb{R} : \Theta \mapsto g(\Theta)$ is the following convex function

$$g(\Theta) := \max_{s \in \mathbb{R}^n} \sum_{t=1}^T \left(\max_{z_t \in \mathbb{R}^d} -C \sum_{i=1}^d l_{ti}^* \left(\frac{-z_{ti}}{C} \right) - \frac{1}{2} (z_t + a_t)^\top \Theta (z_t + a_t) \right). \quad (\text{A.3})$$

Here, $a_t \in \mathbb{R}^d$ for $t = \{1, \dots, T\}$, where $[a_1, \dots, a_T] = \mathcal{A}^*(s)$ and $\mathcal{A}^* : \mathbb{R}^n \rightarrow \mathbb{R}^{d \times T}$ is the adjoint of \mathcal{A} . Furthermore, if Θ^* be the optimal solution of (A.2) and $\{s^*, (z_t^*)_{t=1}^T\}$ be the corresponding optimal solution of (A.3), then the optimal solution $\mathbf{W}^* := [w_1^*, \dots, w_T^*]$ of (A.1) is given by $w_t^* = \Theta^*(z_t^* + a_t^*)$, where $[a_t^*, \dots, a_T^*] = \mathcal{A}^*(s^*)$.

Proof. We derive the Fenchel dual function of $p : \mathbb{R}^{d \times T} \rightarrow \mathbb{R}$,

$$p(\mathbf{W}) = \sum_{t=1}^T \frac{1}{2} w_t^\top \Theta^\dagger w_t + C \sum_{i=1}^d l(y_{ti}, w_{ti}) \quad (\text{A.4})$$

subject to $w_t \in \text{range}(\Theta), \forall t = 1, \dots, T$ and $\mathcal{A}(\mathbf{W}) = \mathbf{0}$, where $\text{range}(\Theta) = \{\Theta z : z \in \mathbb{R}^d\}$. For this purpose, we introduce the auxiliary variables $u_t \in \mathbb{R}^d, \forall t = 1, \dots, T$ which satisfy the constraint $u_{ti} = w_{ti}$. We now introduce the dual variable $z = \{z_1, \dots, z_T\}, z_t \in \mathbb{R}^d$ corresponding to the

constraints $u_{ti} = w_{ti}$, and the dual variable $s \in \mathbb{R}^n$ corresponding to the constraint $\mathcal{A}(\mathbf{W}) = \mathbf{0}$. Then the Lagrangian L of (A.4) is given as:

$$L(\mathbf{W}, u, z, s) = \sum_{t=1}^T \left(\frac{1}{2} w_t^\top \Theta^\dagger w_t + C \sum_{i=1}^d l(y_{ti}, u_{ti}) + \sum_{i=1}^d z_{ti} (u_{ti} - w_{ti}) + i_{\text{range}(\Theta)}(w_t) \right) - \langle s, \mathcal{A}(\mathbf{W}) \rangle. \quad (\text{A.5})$$

where i_H is the indicator function for set H . The dual function q of p is defined as

$$q(z, s) = \min_{\mathbf{W} \in \mathbb{R}^{d \times T}, u_t \in \mathbb{R}^d \forall t} L(\mathbf{W}, u, z, s) \quad (\text{A.6})$$

Using the definition of the conjugate function (Boyd & Vandenberghe, 2004), we get

$$\begin{aligned} \min_{u_t \in \mathbb{R}^d} C \sum_{i=1}^d l(y_{ti}, u_{ti}) + \sum_{i=1}^d z_{ti} u_{ti} &= -C \sum_{i=1}^d \max_{u_{ti} \in \mathbb{R}} \left(\left(-\frac{z_{ti}}{C} \right) u_{ti} - l(y_{ti}, u_{ti}) \right) \\ &= -C \sum_{i=1}^d l_{ti}^* \left(\frac{-z_{ti}}{C} \right), \end{aligned} \quad (\text{A.7})$$

where l_{ti}^* be the Fenchel conjugate function of the loss: $l_{ti} : \mathbb{R} \rightarrow \mathbb{R}$, $v \mapsto l(y_{ti}, v)$.

We next compute the minimizer of L with respect to w_t . From the definition of the adjoint operator, it follows that

$$\langle s, \mathcal{A}(\mathbf{W}) \rangle = \langle \mathcal{A}^*(s), \mathbf{W} \rangle$$

We define $[a_1, \dots, a_T] = \mathcal{A}^*(s)$. Then the Lagrangian L can be re-written as

$$\begin{aligned} L(\mathbf{W}, u, z, s) &= \left(\sum_{t=1}^T \sum_{i=1}^d C l(y_{ti}, u_{ti}) + z_{ti} u_{ti} \right) \\ &+ \sum_{t=1}^T \left(-a_t^\top w_t + \frac{1}{2} w_t^\top \Theta^\dagger w_t + i_{\text{range}(\Theta)}(w_t) - \sum_{i=1}^d z_{ti} w_{ti} \right). \end{aligned}$$

The minimizer of L with respect to w_t satisfy the following conditions

$$\frac{\partial}{\partial w_t} \left(-a_t^\top w_t + \frac{1}{2} w_t^\top \Theta^\dagger w_t - \sum_{i=1}^d z_{ti} w_{ti} \right) = 0, \text{ and} \quad (\text{A.8})$$

$$w_t \in \text{range}(\Theta) \quad (\text{A.9})$$

which implies,

$$\Theta^\dagger w_t = z_t + a_t, \text{ subject to } w_t \in \text{range}(\Theta) \quad (\text{A.10})$$

Thus, the expression of the minimizer of L with respect to w_t is

$$w_t = \Theta(z_t + a_t).$$

Plugging the above result and (A.7) in the dual function (A.6), we obtain

$$q(z, s) = \sum_{t=1}^T \left(-C \sum_{i=1}^d l_{ti}^* \left(\frac{-z_{ti}}{C} \right) - \frac{1}{2} (z_t + a_t)^\top \Theta (z_t + a_t) \right)$$

□

A.2 Proof of Lemma 3

The gradient is computed by employing the Danskin's theorem (Bertsekas, 1999; Bonnans & Shapiro, 2000). The directional derivative of the gradient follows directly from the chain rule.

A.3 Proof of Proposition 1

For convenience, we are reproducing the Proposition 1 from the main paper. Our proposed formulation is

$$\min_{\mathbf{U} \in \mathbb{R}^{d \times r}, \|\mathbf{U}\|_F=1} g(\mathbf{U}\mathbf{U}^\top), \quad (\text{A.11})$$

where the function $g(\mathbf{U}\mathbf{U}^\top)$ is defined as follows, *i.e.*,

$$g(\mathbf{U}\mathbf{U}^\top) := \max_{s \in \mathbb{R}^n} \sum_{t=1}^T \max_{z_t \in \mathbb{R}^d} \left(-C \sum_{i=1}^d l_{ti}^* \left(\frac{-z_{ti}}{C} \right) - \frac{1}{2} \left\| \mathbf{U}^\top (z_t + a_t) \right\|_F^2 \right). \quad (\text{A.12})$$

Proposition 2. *Let $\hat{\mathbf{U}}$ be a feasible solution of (A.11). Then, a candidate solution for (A.2) is $\hat{\Theta} = \hat{\mathbf{U}}\hat{\mathbf{U}}^\top$. Let $\{\hat{s}, (\hat{z}_t)_{t=1}^T\}$ be the optimal solution of the convex problem in (A.12) at $\hat{\mathbf{U}}$. In addition, let σ_1 be the maximum singular of the the matrix whose t^{th} column is $(\hat{z}_t + \hat{a}_t)$, where $[\hat{a}_1, \dots, \hat{a}_T] = \mathcal{A}^*(\hat{s})$. The duality gap (Δ) associated with $\{\hat{\Theta}, \hat{s}, (\hat{z}_t)_{t=1}^T\}$ for (A.2) is given by*

$$\Delta = \frac{1}{2} \left(\sigma_1^2 - \sum_{t=1}^T \left\| \hat{\mathbf{U}}^\top (\hat{z}_t + \hat{a}_t) \right\|^2 \right). \quad (\text{A.13})$$

Proof. Given $\hat{\Theta} = \hat{\mathbf{U}}\hat{\mathbf{U}}^\top$ as described above, the objective value of the min-max problem (A.2) is

$$g(\hat{\Theta}) = -C \sum_{t=1}^T \sum_{i=1}^d l_{ti}^* \left(\frac{-\hat{z}_{ti}}{C} \right) - \frac{1}{2} \sum_{t=1}^T \left\langle \hat{\Theta}, (\hat{z}_t + \hat{a}_t)(\hat{z}_t + \hat{a}_t)^\top \right\rangle. \quad (\text{A.14})$$

Using the min-max interchange (Sion, 1958), the max-min problem corresponding to (A.2) is as follows

$$\max_{s \in \mathbb{R}^n} \max_{z_t \in \mathbb{R}^d \forall t} \left(-C \sum_{t=1}^T \sum_{i=1}^d l_{ti}^* \left(\frac{-z_{ti}}{C} \right) - \frac{1}{2} B \right) \quad (\text{A.15})$$

where

$$B = \max_{\Theta \in \mathcal{P}^d} \left\langle \hat{\Theta}, \sum_{t=1}^T (\hat{z}_t + \hat{a}_t)(\hat{z}_t + \hat{a}_t)^\top \right\rangle. \quad (\text{A.16})$$

Note that problem (A.16) is a well studied problem in the duality theory. It is one of the definitions of the spectral norm (maximum eigenvalue of a matrix) – as the dual of the trace norm (Boyd & Vandenberghe, 2004). Its optimal value is the spectral norm of the matrix $\sum_{t=1}^T (\hat{z}_t + \hat{a}_t)(\hat{z}_t + \hat{a}_t)^\top$ (Boyd & Vandenberghe, 2004). Let σ_1 be the maximum singular of the matrix $E = \sum_{t=1}^T (\hat{z}_t + \hat{a}_t)(\hat{z}_t + \hat{a}_t)^\top$. Then the spectral norm of E is σ_1^2 . Note that the t^{th} column of E is $(\hat{z}_t + \hat{a}_t)$. Putting together the above result, the objective value of the max-min problem, given $\{\hat{s}, (\hat{z}_t)_{t=1}^T\}$ is

$$G = -C \sum_{t=1}^T \sum_{i=1}^d l_{ti}^* \left(\frac{-\hat{z}_{ti}}{C} \right) - \frac{1}{2} \sigma_1^2.$$

Therefore, the duality gap (Δ) associated with $\{\hat{\Theta}, \hat{s}, (\hat{z}_t)_{t=1}^T\}$ for problem (A.2) is given by

$$\begin{aligned} \Delta &= g(\hat{\Theta}) - G \\ &= \frac{1}{2} \left(\sigma_1^2 - \sum_{t=1}^T \left\langle \hat{\Theta}, (\hat{z}_t + \hat{a}_t)(\hat{z}_t + \hat{a}_t)^\top \right\rangle \right) \\ &= \frac{1}{2} \left(\sigma_1^2 - \sum_{t=1}^T \left\| \hat{\mathbf{U}}^\top (\hat{z}_t + \hat{a}_t) \right\|^2 \right) \end{aligned} \tag{A.17}$$

The last equality is obtained by using $\hat{\Theta} = \hat{\mathbf{U}}\hat{\mathbf{U}}^\top$. \square

A.4 Optimization on Spectrahedron

We are interested in the optimization problem of the form

$$\min_{\Theta \in \mathcal{P}^d} f(\Theta), \tag{A.18}$$

where \mathcal{P}^d is the set of $d \times d$ positive semi-definite matrices with unit trace and $f : \mathcal{P}^d \rightarrow \mathbb{R}$ is a smooth function. A specific interest is when we seek matrices of rank r . Using the parameterization $\Theta = \mathbf{U}\mathbf{U}^\top$, the problem (A.18) is formulated as

$$\min_{\mathbf{U} \in \mathcal{S}_r^d} f(\mathbf{U}\mathbf{U}^\top), \tag{A.19}$$

where $\mathcal{S}_r^d := \{\mathbf{U} \in \mathbb{R}^{d \times r} : \|\mathbf{U}\|_F = 1\}$, which is called the spectrahedron manifold (Journée et al., 2010). It should be emphasized the objective function in (A.19) is *invariant* to the post multiplication of \mathbf{U} with orthogonal matrices of size $r \times r$, i.e., $\mathbf{U}\mathbf{U}^\top = \mathbf{U}\mathbf{Q}(\mathbf{U}\mathbf{Q})^\top$ for all $\mathbf{Q} \in \mathcal{O}(r)$, which is the set of orthogonal matrices of size $r \times r$ such that $\mathbf{Q}\mathbf{Q}^\top = \mathbf{Q}^\top\mathbf{Q} = \mathbf{I}$. An implication of this observation is that the minimizers of (A.19) are no longer isolated in the matrix space, but are isolated in the quotient space, which is the set of equivalence classes $[\mathbf{U}] := \{\mathbf{U}\mathbf{Q} : \mathbf{Q}\mathbf{Q}^\top = \mathbf{Q}^\top\mathbf{Q} = \mathbf{I}\}$. Consequently, the search space is

$$\mathcal{M} := \mathcal{S}_r^d / \mathcal{O}(r). \tag{A.20}$$

In other words, the optimization problem (A.19) has the structure of optimization on the *quotient* manifold, i.e.,

$$\min_{[\mathbf{U}] \in \mathcal{M}} f([\mathbf{U}]), \tag{A.21}$$

but numerically, by necessity, algorithms are implemented in the matrix space \mathcal{S}_r^d , which is also called the *total space*.

Below, we briefly discuss the manifold ingredients and their matrix characterizations for (A.21). Specific details of the spectrahedron manifold are discussed in (Journée et al., 2010). A general introduction to manifold optimization and numerical algorithms on manifolds are discussed in (Absil et al., 2008).

A.4.1 Tangent vector representation as horizontal lifts

Since the manifold \mathcal{M} , defined in (A.20), is an abstract space, the elements of its tangent space $T_{[\mathbf{U}]} \mathcal{M}$ at $[\mathbf{U}]$ also call for a matrix representation in the tangent space $T_{\mathbf{U}} \mathcal{S}_r^d$ that respects the equivalence relation $\mathbf{U}\mathbf{U}^\top = \mathbf{U}\mathbf{Q}(\mathbf{U}\mathbf{Q})^\top$ for all $\mathbf{Q} \in \mathcal{O}(r)$. Equivalently, the matrix representation

Table A.1: Matrix characterization of notions on the quotient manifold $\mathcal{S}_r^d/\mathcal{O}(r)$.

Matrix representation of an element	\mathbf{U}
Total space \mathcal{S}_r^d	$\{\mathbf{U} \in \mathbb{R}^{d \times r} : \ \mathbf{U}\ _F = 1\}$
Group action	$\mathbf{U} \mapsto \mathbf{U}\mathbf{Q}$, where $\mathbf{Q} \in \mathcal{O}(r)$.
Quotient space \mathcal{M}	$\mathcal{S}_r^d/\mathcal{O}(r)$
Tangent vectors in the total space \mathcal{S}_r^d at \mathbf{U}	$\{\mathbf{Z} \in \mathbb{R}^{d \times r} : \text{trace}(\mathbf{Z}^\top \mathbf{U}) = 0\}$
Metric between the tangent vector $\xi_{\mathbf{U}}, \eta_{\mathbf{U}} \in T_{\mathbf{U}}\mathcal{S}_r^d$	$\text{trace}(\xi_{\mathbf{U}}^\top \eta_{\mathbf{U}})$
Vertical tangent vectors at \mathbf{U}	$\{\mathbf{U}\mathbf{\Lambda} : \mathbf{\Lambda} \in \mathbb{R}^{r \times r}, \mathbf{\Lambda}^\top = -\mathbf{\Lambda}\}$
Horizontal tangent vectors	$\{\xi_{\mathbf{U}} \in T_{\mathbf{U}}\mathcal{S}_r^d : \xi_{\mathbf{U}}^\top \mathbf{U} = \mathbf{U}^\top \xi_{\mathbf{U}}\}$

of $T_{[\mathbf{U}]}\mathcal{M}$ should be restricted to the directions in the tangent space $T_{\mathbf{U}}\mathcal{S}_r^d$ on the total space \mathcal{S}_r^d at \mathbf{U} that do not induce a displacement along the equivalence class $[\mathbf{U}]$. In particular, we decompose $T_{\mathbf{U}}\mathcal{S}_r^d$ into complementary subspaces, the *vertical* $\mathcal{V}_{\mathbf{U}}$ and *horizontal* $\mathcal{H}_{\mathbf{U}}$ subspaces, such that $\mathcal{V}_{\mathbf{U}} \oplus \mathcal{H}_{\mathbf{U}} = T_{\mathbf{U}}\mathcal{S}_r^d$.

The vertical space $\mathcal{V}_{\mathbf{U}}$ is the tangent space of the equivalence class $[\mathbf{U}]$. On the other hand, the horizontal space $\mathcal{H}_{\mathbf{U}}$, which is any complementary subspace to $\mathcal{V}_{\mathbf{U}}$ in $T_{\mathbf{U}}\mathcal{S}_r^d$, provides a valid matrix representation of the abstract tangent space $T_{[\mathbf{U}]}\mathcal{M}$. An abstract tangent vector $\xi_{[\mathbf{U}]} \in T_{[\mathbf{U}]}\mathcal{M}$ at $[\mathbf{U}]$ has a unique element in the horizontal space $\xi_{\mathbf{U}} \in \mathcal{H}_{\mathbf{U}}$ that is called its *horizontal lift*. Our specific choice of the horizontal space is the subspace of $T_{\mathbf{U}}\mathcal{S}_r^d$ that is the *orthogonal complement* of \mathcal{V}_x in the sense of a *Riemannian metric*.

The Riemannian metric at a point on the manifold is a inner product that is defined in the tangent space. An additional requirement is that the inner product needs to be *invariant* along the equivalence classes (Absil et al., 2008, Chapter 3). One particular choice of the Riemannian metric on the total space \mathcal{S}_r^d is

$$\langle \xi_{\mathbf{U}}, \eta_{\mathbf{U}} \rangle_{\mathbf{U}} := \text{trace}(\xi_{\mathbf{U}}^\top \eta_{\mathbf{U}}), \quad (\text{A.22})$$

where $\xi_{\mathbf{U}}, \eta_{\mathbf{U}} \in T_{\mathbf{U}}\mathcal{S}_r^d$. The choice of the metric (A.22) leads to a natural choice of the metric on the quotient manifold, i.e.,

$$\langle \xi_{[\mathbf{U}]}, \eta_{[\mathbf{U}]} \rangle_{[\mathbf{U}]} := \text{trace}(\xi_{\mathbf{U}}^\top \eta_{\mathbf{U}}), \quad (\text{A.23})$$

where $\xi_{[\mathbf{U}]}$ and $\eta_{[\mathbf{U}]}$ are abstract tangent vectors in $T_{[\mathbf{U}]}\mathcal{M}$ and $\xi_{\mathbf{U}}$ and $\eta_{\mathbf{U}}$ are their horizontal lifts in the total space \mathcal{S}_r^d , respectively. Endowed with this Riemannian metric, the quotient manifold \mathcal{M} is called a *Riemannian quotient manifold* of \mathcal{S}_r^d .

Table A.1 summarizes the concrete matrix operations involved in computing horizontal vectors.

Additionally, starting from an arbitrary matrix (an element in the ambient dimension $\mathbb{R}^{d \times r}$), two linear projections are needed: the first projection $\Psi_{\mathbf{U}}$ is onto the tangent space $T_{\mathbf{U}}\mathcal{S}_r^d$ of the total space, while the second projection $\Pi_{\mathbf{U}}$ is onto the horizontal subspace $\mathcal{H}_{\mathbf{U}}$.

Given a matrix $\mathbf{Z} \in \mathbb{R}^{d \times r}$, the projection operator $\Psi_{\mathbf{U}} : \mathbb{R}^{d \times r} \rightarrow T_{\mathbf{U}}\mathcal{S}_r^d : \mathbf{Z} \mapsto \Psi_{\mathbf{U}}(\mathbf{Z})$ on the tangent space is defined as

$$\Psi_{\mathbf{U}}(\mathbf{Z}) = \mathbf{Z} - \text{trace}(\mathbf{Z}^\top \mathbf{U})\mathbf{U}. \quad (\text{A.24})$$

Given a tangent vector $\xi_{\mathbf{U}} \in T_{\mathbf{U}}\mathcal{S}_r^d$, the projection operator $\Pi_{\mathbf{U}} : T_{\mathbf{U}}\mathcal{S}_r^d \rightarrow \mathcal{H}_{\mathbf{U}} : \xi_{\mathbf{U}} \mapsto \Pi_{\mathbf{U}}(\xi_{\mathbf{U}})$ on the horizontal space is defined as

$$\Pi_{\mathbf{U}}(\xi_{\mathbf{U}}) = \xi_{\mathbf{U}} - \mathbf{U}\mathbf{\Lambda}, \quad (\text{A.25})$$

where $\mathbf{\Lambda}$ is the solution to the *Lyapunov* equation

$$(\mathbf{U}^{\top}\mathbf{U})\mathbf{\Lambda} + \mathbf{\Lambda}(\mathbf{U}^{\top}\mathbf{U}) = \mathbf{U}^{\top}\xi_{\mathbf{U}} - \xi_{\mathbf{U}}^{\top}\mathbf{U}.$$

A.4.2 Retractions from Horizontal Space to Manifold

An iterative optimization algorithm involves computing a search direction (*e.g.*, the gradient direction) and then moving in that direction. The default option on a Riemannian manifold is to move along geodesics, leading to the definition of the exponential map. Because the calculation of the exponential map can be computationally demanding, it is customary in the context of manifold optimization to relax the constraint of moving along geodesics. The exponential map is then relaxed to a *retraction* operation, which is any map $R_{\mathbf{U}} : \mathcal{H}_{\mathbf{U}} \rightarrow \mathcal{S}_r^d : \xi_{\mathbf{U}} \mapsto R_{\mathbf{U}}(\xi_{\mathbf{U}})$ that locally approximates the exponential map on the manifold (Absil et al., 2008, Definition 4.1.1). On the spectrahedron manifold, a natural retraction of choice is

$$R_{\mathbf{U}}(\xi_{\mathbf{U}}) := (\mathbf{U} + \xi_{\mathbf{U}}) / \|\mathbf{U} + \xi_{\mathbf{U}}\|_F, \quad (\text{A.26})$$

where $\|\cdot\|_F$ is the Frobenius norm and $\xi_{\mathbf{U}}$ is a search direction on the horizontal space $\mathcal{H}_{\mathbf{U}}$.

An update on the spectrahedron manifold is, thus, based on the update formula $\mathbf{U}_+ = R_{\mathbf{U}}(\xi_{\mathbf{U}})$.

A.4.3 Riemannian Gradient and Hessian Computations

The choice of the invariant metric (A.22) and the horizontal space turns the quotient manifold \mathcal{M} into a *Riemannian submersion* of $(\mathcal{S}_r^d, \langle \cdot, \cdot \rangle)$. As shown by (Absil et al., 2008), this special construction allows for a convenient matrix characterization of the gradient and the Hessian of a function on the abstract manifold \mathcal{M} .

The matrix characterization of the Riemannian gradient is

$$\text{grad}_{\mathbf{U}} f = \Psi_{\mathbf{U}}(\nabla_{\mathbf{U}} f), \quad (\text{A.27})$$

where $\nabla_{\mathbf{U}} f$ is the Euclidean gradient of the objective function f and $\Psi_{\mathbf{U}}$ is the tangent space projector (A.24).

An iterative algorithm that exploits second-order information usually requires the Hessian applied along a search direction. This is captured by the Riemannian Hessian operator Hess , whose matrix characterization, given a search direction $\xi_{\mathbf{U}} \in \mathcal{H}_{\mathbf{U}}$, is

$$\begin{aligned} \text{Hess}_{\mathbf{U}}[\xi_{\mathbf{U}}] = \Pi_{\mathbf{U}} \Big(& \text{D}\nabla f[\xi_{\mathbf{U}}] - \text{trace}((\nabla_{\mathbf{U}} f)^{\top} \mathbf{U}) \xi_{\mathbf{U}} \\ & - \text{trace}((\nabla_{\mathbf{U}} f)^{\top} \xi_{\mathbf{U}} + (\text{D}\nabla f[\xi_{\mathbf{U}}])^{\top} \mathbf{U}) \mathbf{U} \Big), \end{aligned} \quad (\text{A.28})$$

where $\text{D}\nabla f[\xi_{\mathbf{U}}]$ is the directional derivative of the Euclidean gradient $\nabla_{\mathbf{U}} f$ along $\xi_{\mathbf{u}}$ and $\Pi_{\mathbf{U}}$ is the horizontal space projector (A.25).

Finally, the formulas in (A.27) and (A.28) that the Riemannian gradient and Hessian operations require only the expressions of the standard (Euclidean) gradient of the objective function f and the directional derivative of this gradient (along a given search direction) to be supplied.

A.5 Experiments

In this section, we evaluate the generalization performance as well as computational efficiency of our approach against state-of-the-art in four different applications — matrix completion, robust matrix completion, Hankel matrix learning, and multi-task learning. All our algorithms are implemented using the Manopt toolbox (Boumal et al., 2014). The Matlab codes are available at <https://pratikjawanpuria.com/>.

A.5.1 Matrix Completion

Our first- and second-order methods (Algorithm 1) with square loss are denoted by Proposed-cg-sq and Proposed-tr-sq, respectively.

Baseline techniques: We compare against state-of-the-art fixed-rank and nuclear norm minimization based matrix completion solvers:

- APGL: An accelerated proximal gradient approach for nuclear norm regularization with square loss function (Toh & Yun, 2010).
- Active ALT: State-of-the-art first-order nuclear norm solver based on active subspace selection (Hsieh & Olsen, 2014).
- MMBS: A second-order fixed rank nuclear norm minimization algorithm (Mishra et al., 2013). It employs an efficient factorization of the matrix \mathbf{W} which renders the trace norm regularizer differentiable in the primal formulation.
- R3MC: A non-linear conjugate gradient based approach for fixed rank matrix completion (Mishra & Sepulchre, 2014). It employs a Riemannian preconditioning technique, customized for the square loss function.
- RTRMC: It models fixed rank matrix completion problems with square loss on the Grassmann manifold and solves it via a second order preconditioned Riemannian trust-region method (Boumal & Absil, 2011, 2015).
- LMaFit: A nonlinear successive over-relaxation based approach for low rank matrix completion based on alternate least squares (Wen et al., 2012).
- PRP: a recent proximal Riemannian pursuit algorithm Tan et al. (2016).

Parameter settings: The regularization parameters for respective algorithms are cross-validated in the set $\{1e-6, 1e-5, \dots, 1e0\}$ to obtain their best generalization performance. The optimization strategies for the competing algorithm were set to those prescribed by their authors. For instance, line-search, continuation and truncation were kept on for APGL. The initialization for all the algorithms is based on the first few singular vectors of the given partially complete matrix \mathbf{Y} (Boumal & Absil, 2015). All the fixed algorithms (R3MC, LMaFit, MMBS, RTRMC, Proposed-cg-sq, Proposed-tr-sq) are provided the rank $r = 10$ for real data sets and $r = 5$ for synthetic data set. In all variable rank approaches (APGL, Active ALT, PRP), the maximum rank parameter is set to 10 for real data sets and 5 for synthetic data set. We run all the methods on ten random 80/20 train/test splits and report the average root mean squared error on the test set (test RMSE). We report the minimum test RMSE achieved after the algorithms have converged or have reached maximum number of iterations (`maxIter`). For first-order methods, `maxIter` is set to 500 for the Netflix data set and 200 for other smaller data sets. For second-order methods, `maxIter` is set to 100 for the Netflix data set and 60 for other smaller data sets.

Synthetic data set results. We choose $d = 5\,000$, $T = 500\,000$ and $r = 5$ to create a synthetic data set (with $< 1\%$ observed entries), following the procedure detailed by (Boumal & Absil, 2011, 2015). The number of observed entries for both training ($|\Omega|$) and testing was 15 149 850. The generalization performance of different methods is shown in Figure A.1(a). For the same run, we

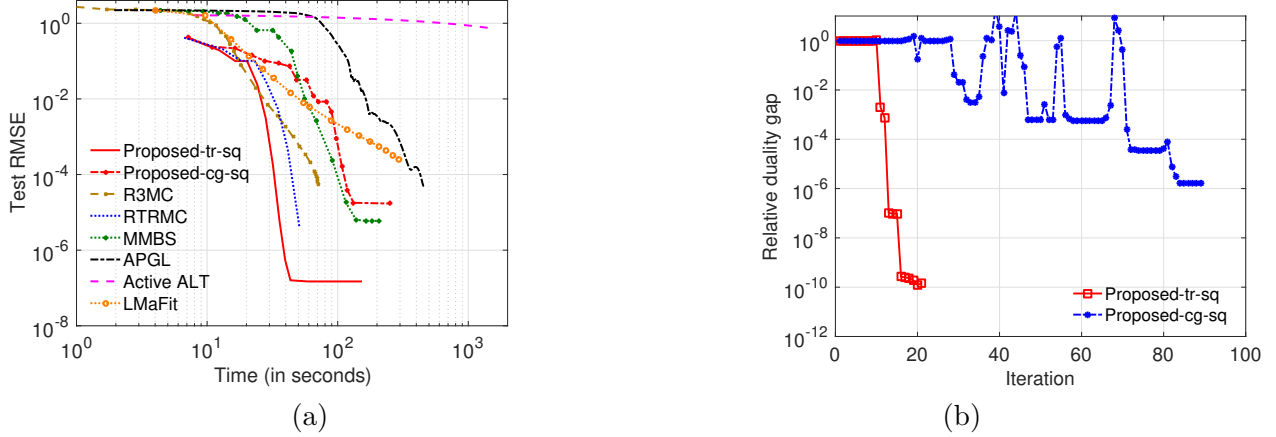


Figure A.1: (a) Evolution of test RMSE on the synthetic data set. Both our methods obtain very low test RMSE; (b) Variation of the relative duality gap per iteration for our methods on the synthetic data set. It can be observed that both our algorithms obtain very low relative duality gap.

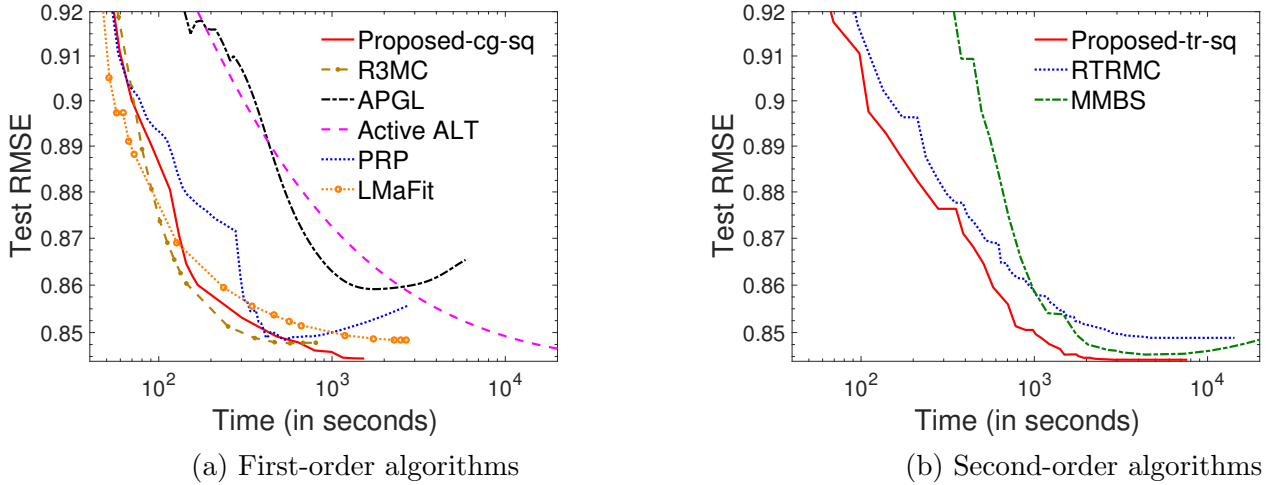


Figure A.2: Evolution of test RMSE on the Netflix data set

Table A.2: Generalization performance of various algorithms on the matrix completion problem. The table reports mean test RMSE along with the standard deviation over ten random train-test split. The proposed algorithms achieve the lowest test RMSE.

	Netflix	MovieLens10m	MovieLens20m
Proposed	0.8443 ± 0.0001	0.8026 ± 0.0005	0.7962 ± 0.0003
Proposed-cg	0.8449 ± 0.0003	0.8026 ± 0.0005	0.7963 ± 0.0003
R3MC	0.8478 ± 0.0001	0.8070 ± 0.0004	0.7982 ± 0.0003
RTRMC	0.8489 ± 0.0001	0.8161 ± 0.0004	0.8044 ± 0.0005
APGL	0.8587 ± 0.0005	0.8283 ± 0.0009	0.8160 ± 0.0013
Active ALT	0.8463 ± 0.0005	0.8116 ± 0.0012	0.8033 ± 0.0008
MMBS	0.8454 ± 0.0002	0.8226 ± 0.0015	0.8053 ± 0.0008
LMaFit	0.8484 ± 0.0001	0.8082 ± 0.0005	0.7996 ± 0.0003
PRP	0.8488 ± 0.0007	0.8068 ± 0.0006	0.7987 ± 0.0008

Table A.3: Data set statistics for the matrix completion application.

	d	T	$ \Omega $
Netflix	17 770	480 189	100 198 805
ML10m	10 677	71 567	10 000 054
ML20m	26 744	138 493	20 000 263

also plot the variation of the relative duality gap across iterations for our methods in figure A.1(b). It can be observed that Proposed-tr-sq approach the global optima for the nuclear norm regularized problem (1) in very few iterations and obtain test RMSE $\approx 2.46 \times 10^{-7}$. Our first order algorithm, Proposed-cg-sq, also achieves lower test RMSE at much faster rate compared to APGL and Active ALT. Note that similar to RTRMC, our methods are able to exploit the condition that $d \ll T$ (rectangular matrices).

Real-world data set results: We tested the methods on three real world data sets: Netflix (Recht & Ré, 2013), MovieLens10m (ML10m) and MovieLens20m (ML20m) (MovieLens, 1997). Their statistics are given in Table A.3. Figures A.2 (a)&(b) display the evolution of root mean squared error on the test set (test RMSE) against the training time on the Netflix data set for first- and second-order algorithms, respectively. Proposed-cg-sq is among the most efficient first-order method and Proposed-tr-sq is the best second-order method. We outperform both APGL and Active ALT, and both our algorithms converge to a lower test RMSE than MMBS at a much faster rate. Table A.2 reports the minimum test RMSE, averaged over ten splits, obtained by all the algorithms on three large-scale real-world data sets: Netflix, MovieLens10m (ML10m), and MovieLens20m (ML20m). Both our algorithms obtain the smallest test RMSE.

A.5.2 Robust Matrix Completion

We compare the following robust matrix completion algorithms: RMC (Cambier & Absil, 2016): state-of-the-art first-order Riemannian optimization algorithm that employs the smooth pseudo-Huber loss function (which successively approximates absolute loss), Proposed-cg-ab: our first-order algorithm with ℓ_1 -loss, and Proposed-cg-svr: our first-order algorithm employing ϵ -SVR loss. It should be emphasized that the non-smooth nature of ℓ_1 -loss and ϵ -SVR loss makes them challenging to optimize in large-scale low-rank settings. All the three loss functions are known to be robust to noise. We follow the same experimental setup described in the previous section.

Figure A.3(a) show the results on the Netflix data set. We observe that both our algorithms scale effortlessly on the Netflix data set, with Proposed-cg-svr obtaining the best generalization result. It should be noted RMC approximates ℓ_1 -loss only towards to the end of its iterations. The test RMSE obtained at convergence are: 0.8685 (Proposed-cg-ab), **0.8565** (Proposed-cg-svr), and 0.8678 (RMC), respectively.

A.5.3 Stochastic system realization (SSR)

Given the observation of noisy system output, the goal in SSR problem is to find a minimal order autoregressive moving-average model (Fazel et al., 2013; Yu et al., 2014). The order of such a model can be shown to be equal to the rank of the Hankel matrix consisting of the exact process covariances (Fazel et al., 2013; Yu et al., 2014). Hence, finding a low-order model is equivalent to learning a low-rank Hankel matrix, while being close to the given data. We perform a small and a large scale experiment in this setting.

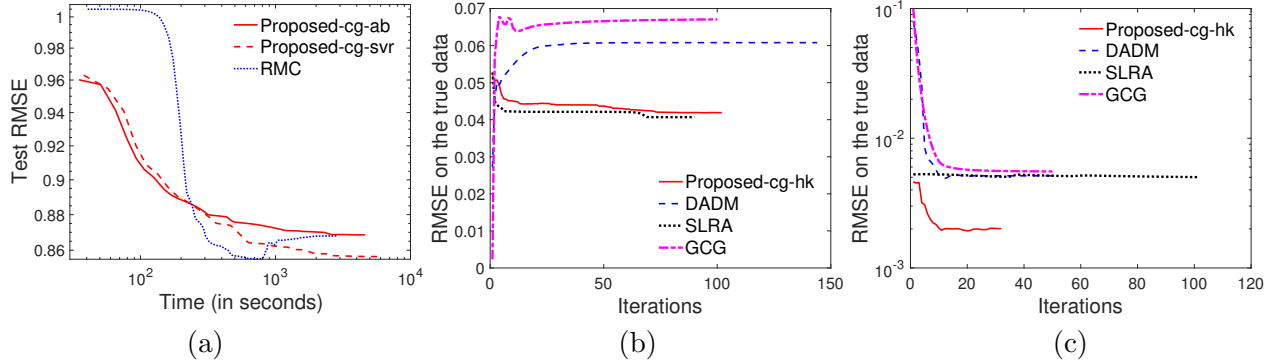


Figure A.3: (a) Evolution of test RMSE of different robust matrix completion algorithms on the Netflix data set; (b) Performance on stochastic system realization problem; (c) Performance on system identification problem;

In our first experiment, the data is generated in accordance with the setting detailed in Fazel et al. (2013); Yu et al. (2014), with $d = 21$, $T = 100$, and $r = 10$. We compare our first-order low-rank Hankel matrix learning algorithm, Proposed-cg-hk, with state-of-the-art solvers GCG (Yu et al., 2014), SLRA (Markovsky, 2014; Markovsky & Usevich, 2014), and DADM (Fazel et al., 2013). We learn a rank-10 Hankel matrix with all the algorithms. Since GCG and DADM have a nuclear norm regularization, we tune their regularization parameter to vary the rank. Proposed-cg-hk is initialized with a random \mathbf{U} matrix, SLRA’s initialization is provided by its authors, and for GCG and DADM, we initialize it with the training matrix. It should be noted that both DADM and GCG are convex approaches and their converged solutions are independent of the initialization. The best result with rank less than or equal to 10 has been reported for GCG and DADM. Figure A.3(b) plots the variation of RMSE with respect to true data (true RMSE) across iterations. It should be noted that the training data is a noisy version of true data. We observe that our algorithm outperforms GCG and DADM and matches SLRA in terms of generalization performance. The true RMSE at convergence is: 0.0419 (Proposed-cg-hk), 0.0671 (GCG), 0.0608 (DADM) and **0.0407** (SLRA). In our second experiment, we generated the data in accordance with the setting detailed in (Markovsky, 2014; Markovsky & Usevich, 2014). We set $d = 1000$, $T = 10000$, and $r = 5$ and repeat the above experiment. The true RMSE is plotted in Figure A.3(c). We observe that our algorithm gives lowest true RMSE.

We also perform experiments on the airline passenger data set (Box & Jenkins, 1990). This is a time-series data set and contains the number of monthly passengers for twelve years. The seasonal variance in the number of monthly passengers possesses the Hankel structure. We learn a rank 10 Hankel matrix (with $d = 11$ and $T = 134$) corresponding to 144 data readings (y). We added Gaussian noise to y to simulate the realistic setting that the vector given to the algorithms has noise. The true RMSE obtained by SLRA, Proposed-cg-Hk, DADM, and GCG are 0.0443, 0.0506, 0.1018, and 0.0773, respectively.

A.5.4 Multi-task Learning

In this experiment, we compare the generalization performance of our multi-task feature learning algorithm Proposed-tr-mtfl (for the formulation in Table 1, row 4) with the convex multi-task feature learning algorithm MTFL (Argyriou et al., 2006, 2008). It should be stated that MTFL solves the convex problem (3) without the $\mathcal{A}(\mathbf{W}) = \mathbf{0}$ constraint optimally via an alternate optimization algorithm. Optimal solution for MTFL at different ranks is obtained by tracing the solution path

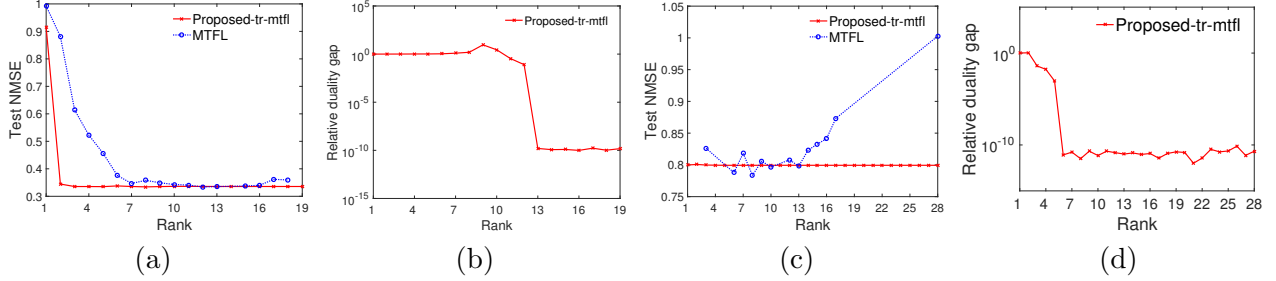


Figure A.4: (a) & (c) Variation of normalized mean squared error (NMSE) as the rank of the optimal solution changes on Parkinsons and School data sets respectively. Our multi-task feature learning method, Proposed-tr-mt, obtains best generalization at much lower rank compared to state-of-the-art MTFL algorithm (Argyriou et al., 2008); (b) & (d) The relative duality gap (Δ) corresponding to the optimal solutions obtained by our method at different ranks. A small Δ implies that our optimal solution is also the optimal solution of the trace norm regularized formulation (1). Figure best viewed in color.

with respect to parameter C , whose value is varied as $\{2^{-8}, 2^{-7}, \dots, 2^{24}\}$. We vary the rank parameter r in our algorithm to obtain different ranked solutions for a given C . The experiments are performed on two benchmark multi-task regression data sets:

- Parkinsons: We need to predict the Parkinson’s disease symptom score of 42 patients (Frank & Asuncion, 2010). Each patient is described using 19 bio-medical features. The data set has a total of 5,875 readings from all the patients.
- School: The data consists of 15,362 students from 139 schools (Argyriou et al., 2008). The aim is to predict the performance of each student given their description and earlier record. Overall, each student data has 28 features. Predicting the performance of students belonging to one school is considered as one task.

Following (Argyriou et al., 2008; Zhang & Yeung, 2010), we report the normalized mean square error over the test set (test NMSE). Figure A.4(a) present the results on the Parkinsons data set. We observe from the figure that our method achieves the better generalization performance at low ranks compared to MTFL. Figure A.4(c) shows similar results on the School data set.